Genetic screen identifies microRNA cluster 99b/let-7e/125a as a regulator of primitive hematopoietic cells

*Alice Gerrits,[1,2] *Marta A. Walasek,[1,2] Sandra Olthof,[1,2] Ellen Weersing,[1,2] Martha Ritsema,[1,2] Erik Zwart,[1,2] Ronald van Os,[1,2] Leonid V. Bystrykh,[1,2] and Gerald de Haan[1,2]

[1]Department of Cell Biology, Section Stem Cell Biology, and [2]European Research Institute on the Biology of Aging, University Medical Center Groningen, University of Groningen, Groningen, The Netherlands

Hematopoietic stem/progenitor cell (HSPC) traits differ between genetically distinct mouse strains. For example, DBA/2 mice have a higher HSPC frequency compared with C57BL/6 mice. We performed a genetic screen for microRNAs that are differentially expressed between LSK, $LS^{-}K^{+}$, erythroid and myeloid cells isolated from C57BL/6 and DBA/2 mice. This analysis identified 131 microRNAs that were differentially expressed between cell types and 15 that were differentially expressed between mouse strains. Of special interest was an evolutionary conserved miR cluster located on chromosome 17 consisting of miR-99b, let-7e, and miR-125a. All cluster members were most highly expressed in LSKs and down-regulated upon differentiation. In addition, these microRNAs were higher expressed in DBA/2 cells compared with C57BL/6 cells, and thus correlated with HSPC frequency. To functionally characterize these microRNAs, we overexpressed the entire miR-cluster 99b/let-7e/125a and miR-125a alone in BM cells from C57BL/6 mice. Overexpression of the miR-cluster or miR-125a dramatically increased day-35 CAFC activity and caused severe hematopoietic phenotypes upon transplantation. We showed that a single member of the miR-cluster, namely miR-125a, is responsible for the majority of the observed miR-cluster overexpression effects. Finally, we performed genome-wide gene expression arrays and identified candidate target genes through which miR-125a may modulate HSPC fate. (*Blood*. 2012;119(2):377-387)

Introduction

HSCs sustain lifelong blood production, and are characterized by their self-renewal capacity and multilineage differentiation potential. HSCs give rise to progenitors that differentiate into the various blood cell types. Many characteristics of the hematopoietic stem and progenitor cell (HSPC) compartment display mouse strain-dependent genetic variation. For example, compared with C57BL/6 (B6) mice, DBA/2 (D2) mice have a higher HSPC frequency and cycling rate.[1-4] The variation between these inbred mouse strains can be exploited to identify potential modulators of such HSPC traits. Useful in this respect has been the generation of BXD recombinant inbred mouse strains.[5,6] Each of these strains represents a unique, but stable, genetic mosaic of B6 and D2 alleles. By making use of these strains, variation in many different HSPC traits has been mapped to genomic regions (reviewed in Gerrits et al[7]). Previously, we analyzed mRNA expression variation in developmentally related cell types isolated from the BXD mouse panel.[8,9] In those studies, we identified groups of genes that were differentially expressed across mouse strains and therefore potentially causal for the variation in HSPC traits.

MicroRNAs are evolutionary conserved small (~ 22-nucleotide) noncoding RNAs that fine-tune gene expression by base-pairing with target mRNAs, leading to mRNA destabilization or translational repression.[10-12] Each microRNA can coordinately target hundreds of different mRNAs,[13] and each mRNA can harbor multiple microRNA target sites, creating complex microRNA/mRNA regulatory circuitries. A growing body of evidence has implicated specific microRNAs in the regulation of HSPC fate. For example, miR-181, miR-150, and the miR-17~92 cluster have proven to be essential for lymphoid development,[14-18] miR-223 for myeloid development,[19,20] and miR-155 for both lymphoid and myeloid development.[21-23] Dysregulated expression of these and other microRNAs has been shown to contribute to the pathogenesis and progression of hematologic malignancies.[24,25]

To determine whether the variation in gene expression and HSPC traits across mouse strains could be due to natural variation in microRNA expression, we initiated a genome-wide microRNA expression study of $Lin^{-}Sca\text{-}1^{+}c\text{-}Kit^{+}$ (LSK), $Lin^{-}Sca\text{-}1^{-}c\text{-}Kit^{+}$ ($LS^{-}K^{+}$), erythroid and myeloid cells isolated from B6 and D2 mice. We identified both cell type–dependent and mouse strain–dependent microRNAs. Interestingly, we discovered an evolutionary conserved cluster of microRNAs (99b/let-7e/125a) that is most highly expressed in HSPCs and that is differentially expressed between mouse strains. To assess whether the differential expression of members of this cluster could be functional, we overexpressed both the entire miR-cluster 99b/let-7e/125a and miR-125a alone in HSPCs, and found that this conferred an initial competitive advantage to these cells. However, we also found that mice reconstituted with these cells developed myeloproliferative neoplasms (MPNs). Our data suggest that miR-125a is responsible for the majority of the hematopoietic effects observed for the entire miR-cluster 99b/let-7e/125a. Finally, we identified the candidate functional downstream targets through which miR-125a may be able to modulate HSPC fate.

Submitted January 20, 2011; accepted November 3, 2011. Prepublished online as *Blood* First Edition paper, November 28, 2011; DOI 10.1182/blood-2011-01-331686.

*A.G. and M.A.W. contributed equally to this work.

The online version of this article contains a data supplement.

The publication costs of this article were defrayed in part by page charge payment. Therefore, and solely to indicate this fact, this article is hereby marked "advertisement" in accordance with 18 USC section 1734.

Methods

Mice

Female B6 (CD45.2) and D2 mice were purchased from Harlan and housed under clean conventional conditions. Female and male B6.SJL (CD45.1) mice were bred at the Central Animal Facility of the University of Groningen. All animal experiments were approved by the Groningen University Animal Care Committee.

Cell purification

BM cells were flushed from the femurs and tibias of 3 to 5 mice and pooled. Nucleated cells were stained with a panel of Alexa Fluor 700 (A700)–labeled lineage-specific Abs, FITC-labeled anti–Sca-1, PE-labeled anti–c-Kit, PE–cyanine-7 (PE-Cy7)–labeled anti–TER-119, and allophycocyanin-labeled anti–Gr-1. Abs were purchased from BioLegend. Triplicates were generated for each of the 8 conditions (4 cell types, 2 mouse strains).

MicroRNA expression analysis

Total RNA was isolated using the miRNeasy Mini Kit (QIAGEN) in accordance with the manufacturer's protocol. Total RNA (100 ng) was labeled and hybridized to Agilent 8 × 15K Mouse miRNA arrays. Labeling, hybridization, and washing were performed by Oxford Gene Technology using the Agilent Mouse microRNA Microarray Kit. Data were extracted using Agilent Feature Extraction Software (Version 9.5.3.1). Data were thresholded at 1, log2-transformed, and normalized to the 75th percentile using GeneSpring GX11.0 (Agilent). On the basis of principal component analysis, 1 sample was removed from further analysis. The starting dataset represented 577 noncontrol probes. False positives were excluded by only pursuing with those probes that were flagged as present in at least 2 of 3 replicates in any 1 of 8 conditions. The quality-filtered expression values were median-centered per microRNA and clustered (Euclidean distance, complete linkage) using Genesis.[26] Two-way ANOVA was applied to identify cell type–dependent and mouse strain–dependent microRNAs. A Benjamini-Hochberg false discovery rate correction was applied to control for multiple testing ($P < .05$). All microarray data are available for viewing on the Gene Expression Omnibus (GEO) under accession number GSE33691.

Retroviral vectors

Genomic DNA was isolated from B6 cells and a 1.2-kb region spanning the miR-99b, let-7e, and miR-125a stem loop sequences was amplified (forward primer: 5′-CCTCGAGTGGACTGAGGAGAATTGAGTGCAAG-3′, reverse primer: 5′-GCAATTGTGCCCTGAAGATCAGCAGGAAC-3′; Biolegio). The resulting PCR product was extracted from gel, TOPO-cloned into PCR4, cut from PCR4 using *Xho*I and *Mun*I, and subcloned into the *Xho*I-*Eco*RI site of the MXW-pPGK-IRES-EGFP vector, which is a murine stem cell virus–based vector with constitutively active PolII type promoter.[27] The miR-125a vector was constructed from the miR-99b/let-7e/125a vector by deleting the *Eco*RI-*Bst*BI fragment (carrying the miR-99b/let7e segment of the miR cluster), followed by vector religation with an aliquot of random hexamers. The miR-155 gene product and the MXW-pPGK-IRES-EGFP vector were a kind gift from Prof Chen (Stanford University School of Medicine, Stanford, CA). The miR-cluster 99b/let-7e/125a, miR-125a and miR-155 fragments were sequence verified (StarSeq; see supplemental Methods, available on the *Blood* Web site; see the Supplemental Materials link at the top of the online article).

Retroviral overexpression of microRNAs in primary BM cells

Primary BM cells were isolated from B6 mice 4 days after IP injection of 150 mg/kg 5-fluorouracil (Pharmachemie Haarlem), and cultured in StemSpan (StemCell Technologies) supplemented with 10% FCS, 300 ng/mL recombinant mouse SCF (rmSCF; Peprotech), 20 ng/mL rmIL11 (R&D Systems), 1 ng/mL Flt3 ligand (Amgen), penicillin, and streptomycin. BM cells were transduced by transfecting Phoenix ecotropic packaging cells with 1-2 μg of pDNA (MXW empty vector, MXW-miR-cluster 99b/let-7e/125a, MXW-miR-125a, and MXW-miR-155) and 3-6 μL of Fugene HD (Roche). Virus-containing supernatant harvested 48 and 72 hours later was used to transduce 4-6 × 10^5 BM cells per 3.5-cm well. Three independent transductions were performed per condition per experiment. Five days after the first transduction, viable (negative for propidium iodide) EGFP$^+$ cells were collected and tested in in vitro assays and collected in RNA lysis buffer (QIAGEN) for gene expression studies. Nonsorted cells were tested in an in vivo BM transplantation setting.

Quantitative PCR validation

We converted selected microRNAs to cDNA using the TaqMan MicroRNA Reverse Transcription Kit (Applied Biosystems). Next, real-time PCR with TaqMan MicroRNA assays (Applied Biosystems) was performed using the iCycler system (Bio-Rad). The following assays were used: hsa-miR-99b, hsa-let-7e, hsa-miR-125a-5p, mmu-miR-155, and snoRNA202. The comparative $\Delta\Delta C_t$ approximation method was used to analyze relative changes in gene expression.[28] Each of the 3 samples was analyzed in triplicate and normalized to the endogenous control snoRNA202.

CAFC assays

The cobblestone-area forming cell (CAFC) assay was performed as previously described.[29,30]

Primary BM transplantation

BM cells were transplanted into lethally irradiated recipients without prior sorting for EGFP expression. Two independent transplantation experiments were performed, where B6 and B6.SJL mice were exchangeably used as a source of donor cells or transplant recipients. In both experiments, 9 mice (3 independent transductions × 3 mice) received transplants per condition with 5-10 × 10^6 cells each. On a 4- to 6-week basis posttransplantation blood analyses were performed. Blood cell numbers were counted using a Medonic hematology analyzer (Boule Medical). Subsequently, cells were stained with PE-labeled anti-CD45.2, Pacific Blue–labeled anti-CD45.1, allophycocyanin-Cy7–labeled anti–Gr-1, PE-Cy7–labeled anti-CD11b, Pacific Orange–labeled anti-CD45R/B220 (Invitrogen, Caltag Laboratories), and allophycocyanin-labeled anti-CD3ϵ. Abs were purchased from BioLegend, unless otherwise specified. Data were acquired using an LSR II (BD Biosciences) and analyzed using FlowJo software (TreeStar). At the time of sacrifice, the peripheral blood, BM, spleen, liver, and in a few instances, lung tissues were analyzed. Cell counts, cytospin preparations, and FACS stainings were performed. Cells were stained using the aforementioned Abs mix or stained with lineage cocktail (A700-labeled anti-Mac1, A700-labeled anti–Gr-1, A700-labeled anti–TER-119, A700-labeled anti-CD3ϵ, A700-labeled anti-B220), PE-labeled anti-cKit, Pacific Blue–labeled anti–Sca-1, PE-Cy7–labeled anti-CD150 and A647-labeled anti-CD48. Cytospins were stained with May-Grünwald-Giemsa (MGG).

Secondary BM transplantation

EGFP$^+$CD45.2$^+$ BM cells from the primary miR cluster and empty vector mice received transplants in competition with freshly isolated wild-type CD45.1$^+$ BM cells in lethally irradiated recipients (CD45.2) at 4:1 (test to freshly isolated) ratios. For each of the conditions, 15 mice (3 individual primary mice × 5 secondary mice) received transplants with a total of 5 × 10^6 cells each. Blood analyses were performed on a 4- to 6-week basis posttransplantation.

Downstream target analysis

Genome-wide gene expression was profiled in BM cells transduced with empty vector, miR-cluster 99b/let-7e/125a, miR-125a, and miR-155. Heterogeneous populations of viable EGFP$^+$ BM cells were FACS-purified without any additional marker selection at 5 days after the first transduction (the exact time point at which the aforementioned in vitro and in vivo assays were initiated). All samples were analyzed in triplicate. Total RNA was isolated using the RNeasy Mini Kit (QIAGEN). RNA was amplified using

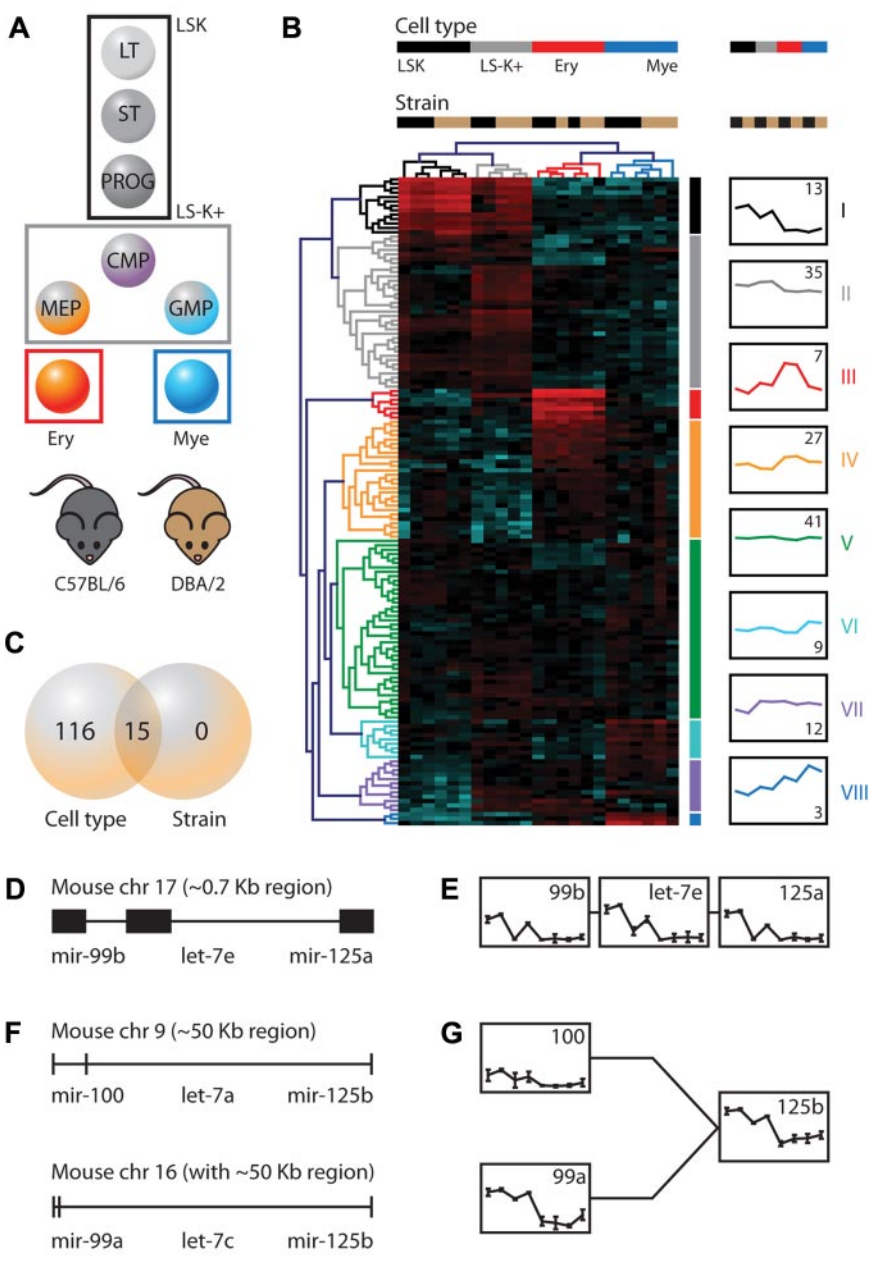

Figure 1. Genetic screen identifies cell type– and mouse strain–dependent microRNAs. (A) MicroRNA expression was evaluated in 4 developmentally related cell types isolated from the BM of C57BL/6 and DBA/2 mouse strains. (B) Hierarchical clustering was performed using the 147 quality-filtered probes (Euclidean distance, complete linkage). Samples are in columns, microRNAs in rows. For each probe, data were median-centered, with the lowest and highest intensity values in blue and red, respectively. Of each of the 8 microRNA signatures the average expression across cell types and mouse strains is shown (y-axis represents log2 expression ranging from −4 to 8). The number in the graphs indicates the number of microRNAs per signature. (C) Venn diagram showing the number of differentially expressed microRNAs between cell types and mouse strains. (D) An evolutionary conserved microRNA cluster, consisting of miR-99b, let-7e, and miR-125a, located on mouse chromosome 17. (E) Expression of miR-cluster 99b/let-7e/125a members across cell types and mouse strains (axes: as in panel B). Shown is the mean ± SD. (F) Paralogous microRNA clusters on chromosomes 9 and 16. (G) Expression of miR-100, miR-99a, and miR-125b across cell types and mouse strains (axes: as in panel B). For miR-125b only the cumulative expression of the chromosome 9 and 16 cluster could be assessed. Expression of let-7a and let-7c is not shown, as only the cumulative expression from multiple different genomic locations (including other chromosomes than 9, 16, and 17) could be assessed. Shown is the mean ± SD. LT indicates long-term; ST, short-term; CMP, common myeloid progenitor; MEP, megakaryocyte-erythrocyte progenitor; and GMP, granulocyte-macrophage progenitor.

the Illumina TotalPrep RNA Amplification Kit (Ambion/Applied Biosystems) and hybridized to Sentrix MouseWG-6 Version 2.0 expression beadchips (Illumina) according to the manufacturer's instructions. Hybridization and washing were performed by our in-house Genome Analysis Facility. Scanning was carried out on the iScan System (Illumina). Data were extracted using GenomeStudio software (Illumina), without normalization or background subtraction. Data were thresholded at 1, log2-transformed, and quantile normalized using GeneSpring GX11.0 (Agilent). The starting dataset represented 45.281 probes. False positives were excluded by only pursuing with those probes that were flagged as marginal or present in all replicates in any 1 of 4 conditions (default detection *P* values cutoff 0.8 for present and 0.6 for absent were used for flags). Predicted (conserved) downstream microRNA targets were imported from the TargetScan database.[31]

URLs

All raw data were deposited in the NCBI Gene Expression Omnibus (GEO, http://www.ncbi.nlm.nih.gov/geo/, accession number GSE33691). All processed microRNA expression data on the 4 cell types from B6 and D2 mice were deposited on HemDb (http://hemdb.org/).

Results

Identification of cell type–dependent microRNA signatures

To identify cell type–dependent and mouse strain–dependent micro-RNAs in the hematopoietic system, we started a microarray-based microRNA profiling study of 4 developmentally related hematopoietic cell types isolated from the BM of B6 and D2 mice. We hybridized total RNA isolated from purified LSK multilineage cells, committed $LS^{-}K^{+}$ cells, erythroid TER-119^{+} cells, and myeloid Gr-1^{+} cells (Figure 1A) to Agilent microRNA arrays and evaluated microRNA expression levels. In total, we analyzed 23 samples representing 4 different cell types and 2 different mouse strains. Of the 577 microRNAs profiled, 147 were expressed in at

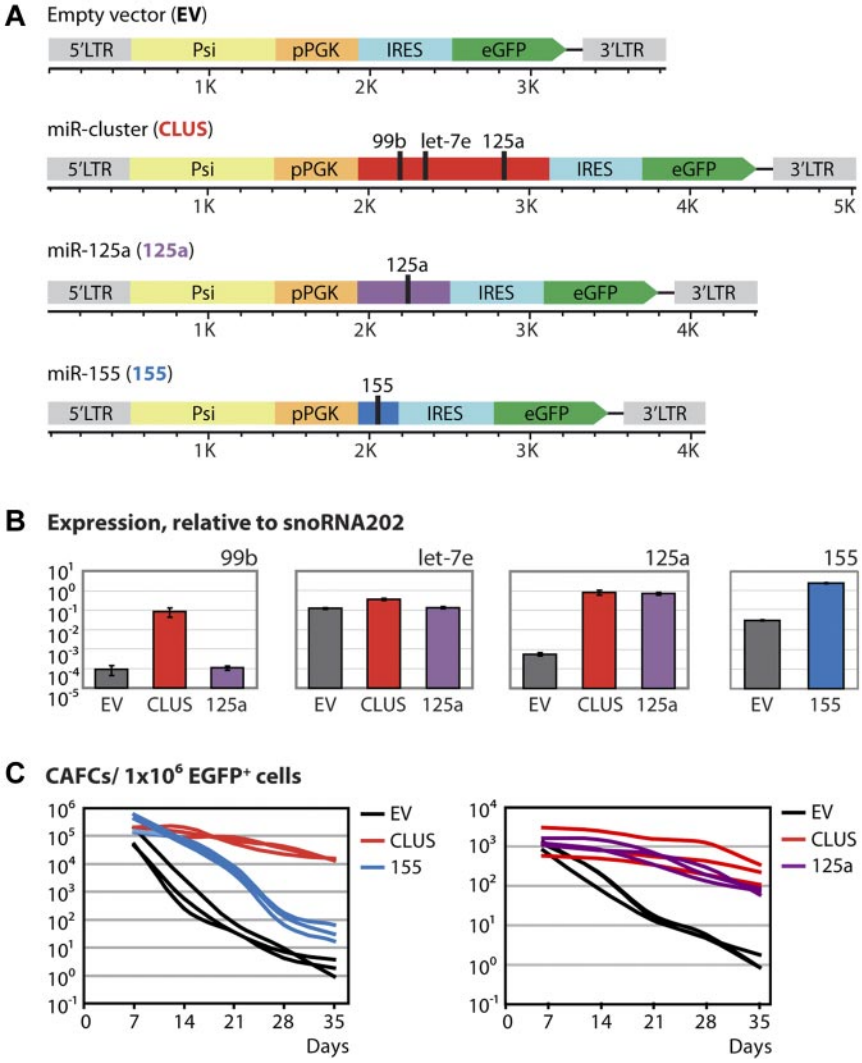

Figure 2. Overexpression of miR-cluster 99b/let-7e/125a or miR-125a alone fixes HSPCs in a primitive state. (A) Schematic representation of the retroviral vectors used to overexpress miR-cluster 99b/let-7e/125a, miR-125a and miR-155. (B) Quantitative RT-PCR data showing the expression levels of the miR-cluster 99b/let-7e/125a members and miR-155 on overexpression relative to the endogenous control snoRNA202. Shown is the mean ± SD. (C) CAFC data showing the number of HSPCs.

least 1 of these 8 conditions. To study the relationship between the samples, as well as the underlying patterns of microRNA expression, we applied an unsupervised 2-way hierarchical clustering method using the 147 quality-filtered microRNAs. This analysis showed that the cell-type effect greatly exceeded the mouse strain effect (Figure 1B top tree), and revealed 8 distinct microRNA signatures (Figure 1B left tree; supplemental Table 1). Of special interest is signature I consisting of microRNAs that are most highly expressed in LSKs and down-regulated upon differentiation. Signature I consists of miR-125a-5p, miR-125b-5p, miR-126-3p, miR-130a, miR-155, miR-181d, miR-196b, miR-203, miR-222, miR-31, miR-99a, miR-99b, and let-7e. Considering their expression pattern, these microRNAs may represent important factors that keep cells from leaving the stem cell state. Signature II consists of microRNAs that are most highly expressed in $LS^{-}K^{+}$ cells, signatures III and IV are specific to erythroid cells, and signatures VI and VIII to myeloid cells. Signature VII consists of microRNAs that are expressed in all cell types except for LSKs, and may therefore consist of microRNAs that are important for lineage specification, commitment, and differentiation. Finally, signature V does not show a clear expression preference. We confirmed well-known cell-type–specific microRNAs: eg miR-196b in signature I,[32] miR-451 in erythroid signature III,[33] and miR-223 in myeloid signature VIII.[19,20] The entire microRNA expression dataset is available online (supplemental Table 1 and in GEO [accession number GSE33690]), and queries for specific microRNAs can be done on www.hemdb.org.

Identification of mouse strain–dependent miR-cluster 99b/let-7e/125a

An analysis of variance (2-way ANOVA, corrected $P < .05$) yielded 131 differentially expressed microRNAs, all of which showed a cell-type effect and of which 15 also showed a mouse strain effect (Figure 1C, supplemental Table 1). In total, 4 of the 15 mouse strain–dependent microRNAs were present in signature I, namely miR-125a, miR-125b, miR-130a, and miR-99b. They were all most highly expressed in the primitive cell compartment and down-regulated upon differentiation and generally higher expressed in D2 cells compared with B6 cells. These 2 criteria qualify those microRNAs as potential candidates regulating HSPC traits. Interestingly however, 2 of these 4, miR-125a and miR-99b are part of an evolutionary conserved microRNA cluster that is localized on chromosome 17: miR-cluster 99b/let-7e/125a (Figure 1D). The third member of this cluster, let-7e, shows an expression pattern comparable with the other 2 members (Figure 1E), but its strain effect did not reach statistical significance (corrected $P = .064$). In addition, miR-125b is present in 2 paralogous microRNA clusters that are located on chromosomes 9 and 16 (Figure 1F). The chromosome 9 cluster consists of miR-100, let-7a,

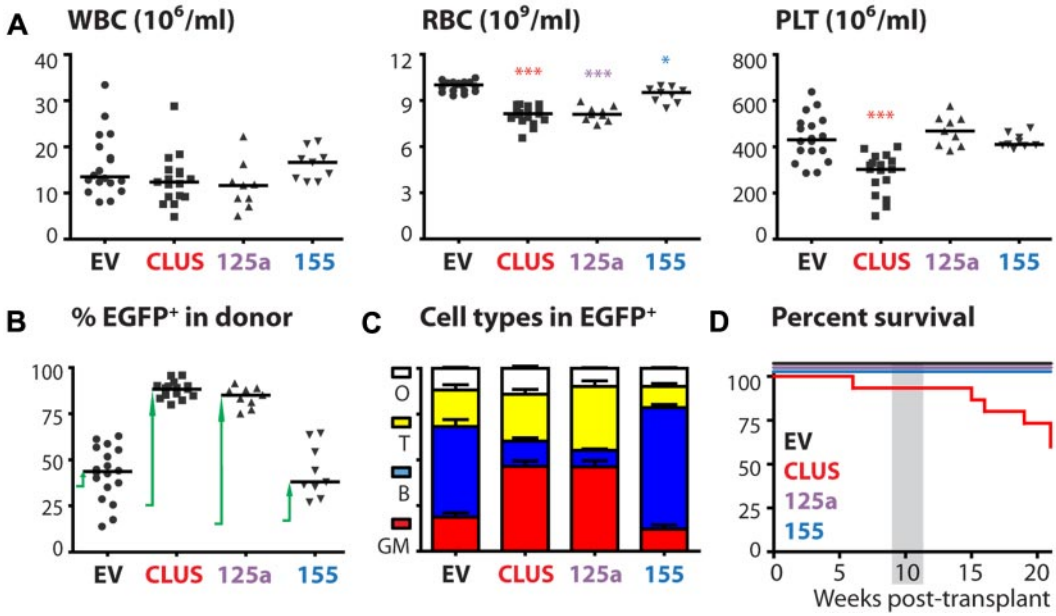

Figure 3. Sustained expression of miR-cluster 99b/let-7e/125a or miR-125a alone disturbs hematopoiesis. (A) WBC, RBC, and platelet counts at 10 weeks after transplantation (n = 9-18 mice/group). *P* values (*.01 < *P* < .05; ***P* < .001) are displayed (Mann-Whitney test). (B) Chimerism levels were assessed at 10 weeks after transplantation by analyzing the percentage of EGFP⁺ cells in the donor fraction (n = 9-18 mice/group). The arrows indicate the increase in chimerism levels over the first 10 weeks after transplantation. (C) Cell-type distribution in the blood as assessed by FACS (n = 9-18 mice/group). Shown is the mean ± SEM (D) Survival of mice (n = 9-18 mice/group). The gray box indicates the time point analyzed in the other panels. WBC indicates white blood cells; RBC, red blood cells; PLT, platelets; GM, granulocytes/macrophages; B, B lymphocytes; T, T lymphocytes; and O, other cell types.

and miR-125b-1 and the chromosome 16 cluster consists of miR-99a, let-7c, and miR-125b-2. Although not all microRNA cluster members display a significant mouse strain effect, they all follow the same expression trend across cell types and mouse strains (Figure 1G). This view corroborates previous observations that proximal pairs of microRNAs (separated by < 50 kb) are generally coexpressed across tissues.[34]

Overexpression of miR-cluster 99b/let-7e/125a or miR-125a alone retains HSPCs in a primitive state

To assess whether differential expression of members of the 99b/let-7e/125a microRNA cluster could have functional consequences for HSPCs, and could be causal for the phenotypic differences between HSPCs from B6 and D2 mice, we performed gain-of-function studies. We cloned the entire 99b/let-7e/125a cluster, as these 3 microRNAs showed coordinated expression, and miR-125a alone in a retroviral vector (both in its natural genomic context) (Figure 2A). MiR-155, known to affect HSPC characteristics, was included as a positive control.[21] The miR-cluster 99b/let-7e/125a, miR-125a, and miR-155 were overexpressed in BM cells from 5-FU–treated mice. Transduced cells were sorted and overexpression of the individual members of miR-cluster 99b/let-7e/125a and miR-155 was validated using quantitative PCR (Figure 2B). Engineered expression levels of miR-cluster 99b/let-7e/125a members were substantially increased (1000-, 2-, 1500-fold, respectively) compared with the natural situation, in which members of the miR-cluster are on average 2-fold higher expressed in D2 than in B6 LSK cells (microarrays and quantitative PCR; data not shown). Concurrently, transduced EGFP⁺ cells were used to initiate CAFC, a surrogate in vitro assay to quantify the number of HSPCs. In this assay, early appearing cobblestones (day 7) are considered to represent progenitors and late-appearing cobblestones (day 35) are considered to represent stem cells.[29,30] Day-7 CAFC activity showed no differences between the control and microRNA-overexpressing cells. However, at day 35, a striking difference in the number of CAFCs was observed. The miR-155–overexpressing cells gave ~ 15-fold more CAFCs, whereas the miR-cluster 99b/let-7e/125a–overexpressing cells yielded a striking ~ 6.500-fold more CAFCs (Figure 2C left). Direct comparison between miR-cluster 99b/let-7e/125a and miR-125a alone revealed very similar CAFC activity profiles and no significant differences were observed between these 2 overexpression conditions. Both the miR-cluster 99b/let-7e/125a and miR-125a strongly increased day-35 CAFC activity (Figure 2C right). Moreover, for both the miR-cluster and miR-125a, a substantial amount of CAFC activity remained even up until day 70 (data not shown).

To summarize, BM cells overexpressing miR-cluster 99b/let-7e/125a, miR-125a, or miR-155 showed increased stem cell activity as measured by day-35 CAFC activity. These data suggest that overexpression of miR-cluster 99b/let-7e/125a or miR-125a alone retains cells in a primitive state.

Sustained expression of miR-cluster 99b/let-7e/125a or miR-125a in HSPCs provides a competitive advantage, but also results in MPNs

We next assayed the microRNA-overexpressing cells in a long-term competitive repopulation experiment in vivo. To achieve this, miR-cluster 99b/let-7e/125a, miR-125a alone and miR-155 were overexpressed in BM cells derived from 5-FU–treated mice and nonsorted cells were transplanted into lethally irradiated recipients. At 10 weeks posttransplantation, blood cell counts revealed a significant decrease in RBC numbers and a slight decrease in white blood cell (WBC) numbers for mice transplanted with miR-cluster 99b/let-7e/125a or miR-125a–overexpressing cells. However, whereas platelet counts were significantly decreased in miR-cluster reconstituted mice, this was not observed for miR-125a reconstituted mice. Recipients transplanted with miR-155 transduced cells showed a less dramatic decrease of RBC counts with no effect on WBC and platelet counts (Figure 3A). At this point in time, chimerism was assessed by quantifying the percentage of EGFP⁺

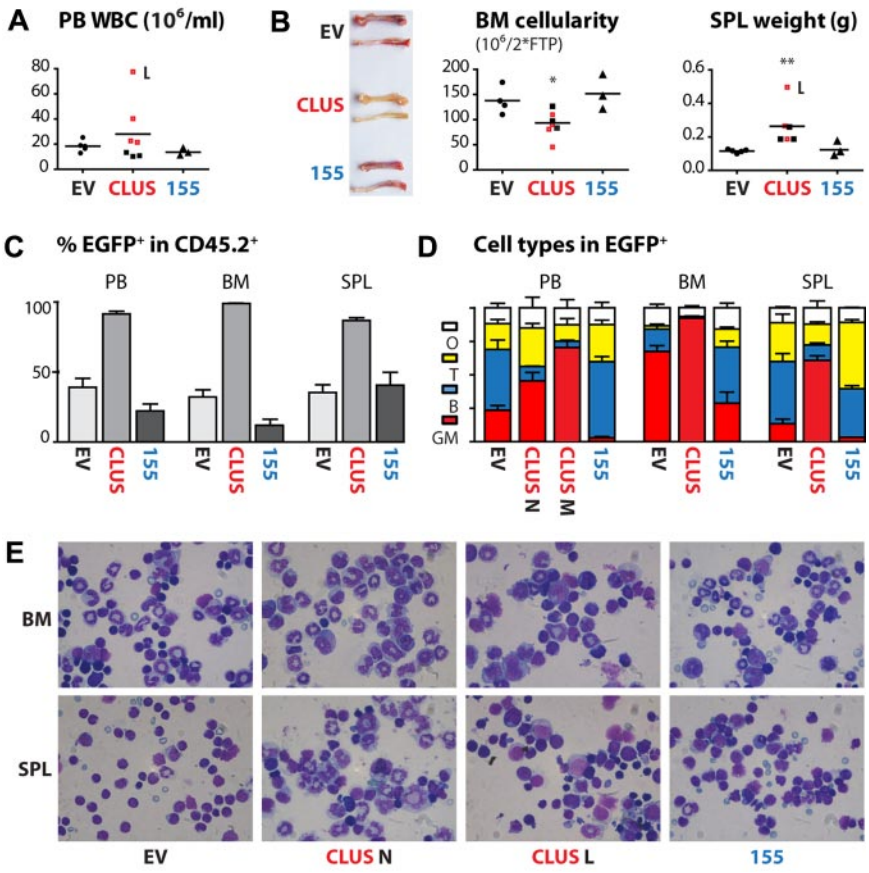

Figure 4. Sustained expression of miR-cluster 99b/let-7e/125a induces MPNs with occasional progression to leukemia. (A) PB WBC counts for empty vector, miR-cluster 99b/let-7e/125a, and miR-155 mice at time of sacrifice. Closed/black squares represent nonmorbid miR-cluster mice, whereas open/red squares represent moribund miR-cluster mice. L indicates leukemic mouse. (B) Photographs of femur and tibia bones, BM cellularity (representing 2 femurs, 2 tibias and pelvic bones) and spleen weight for empty vector, miR-cluster 99b/let-7e/125a and miR-155 mice at time of sacrifice. Closed/black squares represent nonmorbid miR-cluster mice, whereas open/red squares represent moribund miR-cluster mice. *P* values (*.01 < *P* < .05; **.001 < *P* < .01) are displayed (Mann-Whitney test). L indicates leukemic mouse. (C) Percentage EGFP⁺ cells in PB, BM, and spleen (n = 5 for EV, n = 6 for CLUS, n = 3 for 155). Nonmorbid and moribund miR-cluster 99b/let-7e/125a mice showed similar percentages and were therefore combined. Shown is the mean ± SEM. (D) Cell-type distribution in PB, BM, and spleen of empty vector, miR-cluster 99b/let-7e/125a, and miR-155 mice as assessed by FACS. Shown is the mean ± SEM. Data for nonmorbid and moribund mice are shown separately for PB (n = 5 for EV, n = 3 for nonmorbid [N] CLUS, n = 3 for moribund [M] CLUS, n = 3 for 155) and combined for BM and spleen (n = 5 for EV, n = 6 CLUS, n = 3 for 155), because the cell-type distributions between these mice differed in PB, but not in BM and spleen. (E) Representative MGG-stained cytospin preparations from BM and spleen cells. For the miR-cluster 99b/let-7e/125a, 2 pictures are shown: 1 representative of a nonmorbid mouse (N) and 1 of the leukemic mouse (L).

cells within the donor fraction. Whereas within 10 weeks the chimerism levels of the control mice remained relatively stable at 36%, those of the miR-155 mice increased from 15% to 45%, and those of the miR-cluster 99b/let-7e/125a and miR-125a mice increased from 25% or 10%, respectively, to 90%. This indicates that in the latter 3 cases the microRNA-transduced cells had a competitive advantage over the nontransduced cells (Figure 3B). Detailed FACS analyses revealed that the EGFP$^+$ cells in both the miR-cluster 99b/let-7e/125a and miR-125a mice were enriched for granulocytes/macrophages (defined as being Gr-1$^+$ and/or Mac-1$^+$) at the expense of the number of B lymphocytes (B220$^+$; Figure 3C). Clearly, hematopoiesis was disturbed in these mice, resulting in lethality of some of the recipients (Figure 3D). In 1 of 2 independent transplantation experiments, 6 of 9 miR-cluster 99b/let-7e/125a–overexpressing mice died between 6-30 weeks posttransplantation. In the other transplantation experiment, despite strongly disturbed hematopoietic homeostasis of miR-cluster 99b/let-7e/125a and miR-125a mice, no lethality was observed until 21 weeks posttransplantation.

To obtain more insight into the type of hematologic malignancy in the miR-cluster 99b/let-7e/125a–overexpressing mice, we performed pathologic analyses on 3 mice before the onset of morbidity at 21 weeks after transplantation and on 4 mice when they were moribund (6, 16, 19, and 21 weeks after transplantation). Two miR-cluster mice were found dead at 15 and 30 weeks, preventing determination of the cause of death. We compared our findings with analyses on mice reconstituted with empty vector and miR-155–transduced cells. The peripheral blood analyses revealed that all the moribund mice displayed higher WBC counts compared with the nonmorbid mice. Among these moribund mice, there was one clearly leukemic (and one potentially preleukemic) mouse, characterized by high WBC numbers (Figure 4A), splenomegaly (Figure 4B), and large numbers of blast cells in the BM compartment (Figure 4E). Compared with the empty vector mice, the miR-cluster 99b/let-7e/125a mice had pale bones, lower BM cellularities, and increased spleen sizes (Figure 4B). Subsequent FACS analyses revealed that the PB, BM, and spleens of the mice were dominated by EGFP$^+$ cells (Figure 4C) that were mostly of myeloid (defined as being Gr-1$^+$ and/or Mac-1$^+$) origin (Figure 4D). This latter finding was corroborated by morphologic analyses of MGG-stained cytospin preparations (Figure 4E). The livers and lungs of the mice were also infiltrated by these EGFP$^+$ myeloid cells (data not shown).

Taken together, these data show that the miR-cluster 99b/let-7e/125a and miR-125a mice suffered from MPNs that in rare cases progressed to leukemia. In the miR-155 mice, an opposite phenotype could be observed, as the EGFP$^+$ cells in the PB, BM, and spleens of these mice were mostly of lymphoid (defined as being B220$^+$ or CD3$^+$) origin (Figure 4D-E).

Competitive advantage provided by miR-cluster 99b/let-7e/125a decreases over time

To quantify the number of HSPCs in the BM compartments of the nonmorbid miR-cluster 99b/let-7e/125a mice and their empty vector controls, CAFC assays on EGFP$^+$ BM cells were performed. At 21 weeks posttransplantation, the miR cluster–transduced cells still exhibited more day-35 CAFC activity compared with empty vector-transduced cells (Figure 5A). However, it should be noted that the fold increase in day-35 CAFC activity of miR-cluster 99b/let-7e/125a–overexpressing cells dropped from ~ 6.500 before transplantation to ~ 400 in this 21-week time

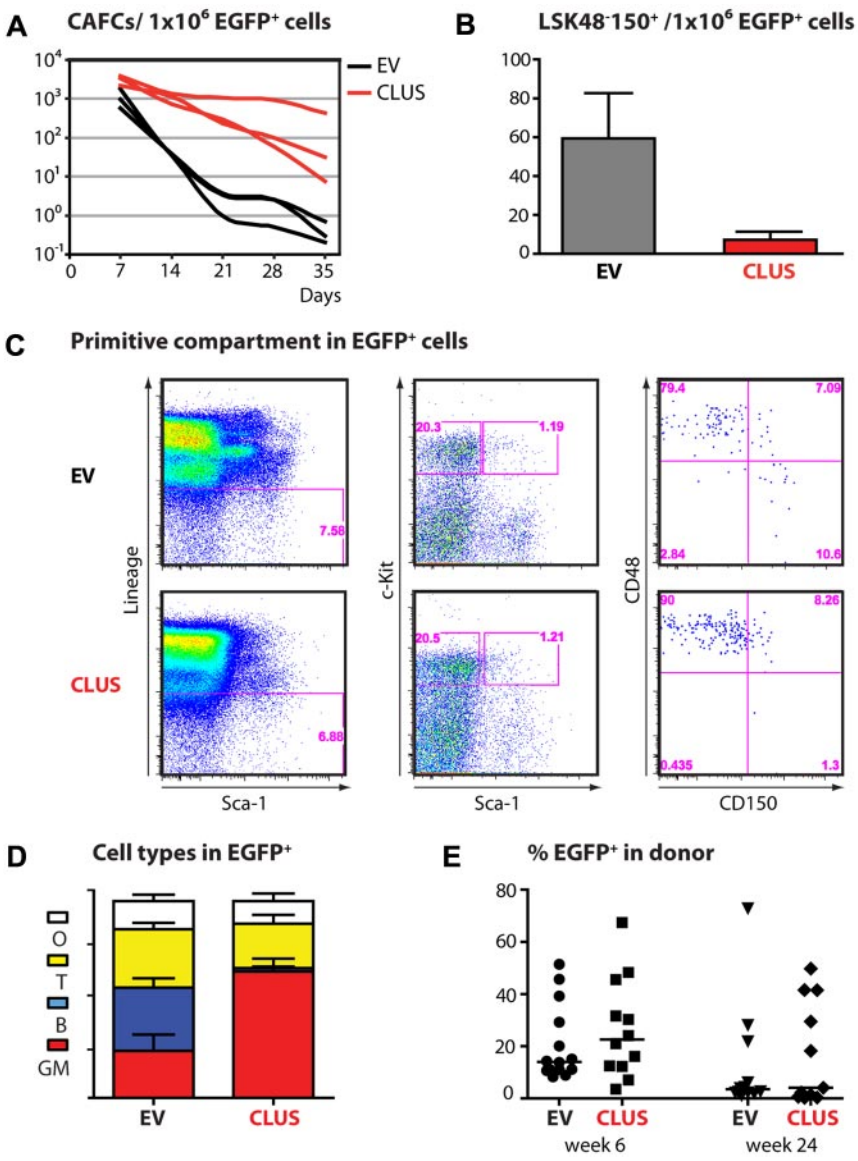

Figure 5. Effects of sustained expression of miR-cluster 99b/let-7e/125a on the stem cell compartment. (A) CAFC data showing the number of HSPCs in the EGFP$^+$ BM fraction of 3 individual empty vector and (nonmorbid) miR-cluster 99b/let-7e/125a mice at $\sim$ 21 weeks posttransplantation. (B) Frequency of LT-HSCs (Lin$^-$Sca-1$^+$c-Kit$^+$CD48$^-$CD150$^+$) per 1×10^6 EGFP$^+$ BM cells at 21 weeks posttransplantation. Analyses were performed using FlowJo software (TreeStar), followed by quantification of the number of LT-HSCs (n = 3/group, same mice as described in panel A). Shown is the mean $\pm$ SEM. (C) Representative FACS plots of the EGFP$^+$ primitive BM compartment at 21 weeks after primary transplantations. (D) Cell-type distribution in the blood of empty vector and miR-cluster 99b/let-7e/125a mice upon secondary transplantations as assessed by FACS at 24 weeks posttransplantation. Shown is the mean $\pm$ SEM (n = 15 mice/group). (E) Chimerism levels at 6 and 24 weeks after secondary transplantation (n = 15 mice/group). GM indicates granulocytes/macrophages; B, B lymphocytes; T, T lymphocytes; and O, other cell types.

frame in vivo. Reduction of the stem cell pool was also suggested by immunophenotypic analyses of the primitive BM compartment. We observed a reduced frequency of EGFP$^+$ primitive stem cells in the BM, defined as Lin$^-$Sca-1$^+$c-Kit$^+$CD48$^-$CD150$^+$ cells, in miR-cluster 99b/let-7e/125a mice compared with empty vector mice 5 months after transplantation (Figure 5B-C).

To assess the quality of the HSPCs in the BM compartments of the miR-cluster 99b/let-7e/125a and empty vector mice, we performed secondary BM transplantations. We evaluated the in vivo repopulating ability of EGFP$^+$ cells isolated from the BM of the primary recipients by transplanting them in competition with freshly isolated BM cells. Whereas miR-cluster 99b/let-7e/125a-overexpressing cells continued to show disturbed hematopoietic homeostasis, reflected by myeloproliferation in the peripheral blood at the expense of the number of B lymphocytes (Figure 5D), their initial competitive advantage was lost. No differences in EGFP$^+$ donor cell chimerism were observed between miR-cluster 99b/let-7e/125a and empty vector mice 6 weeks or 24 weeks after transplantation (Figure 5E).

To summarize, our data indicate that miR-cluster 99b/let-7e/125a indeed affects HSPC traits. We found that overexpression of this microRNA cluster conferred an apparent initial competitive advantage to engrafting hematopoietic cells in an in vivo transplant setting.

In search of functional miR-125a targets

To understand the molecular mechanisms by which miR-cluster 99b/let-7e/125a, and more specifically miR-125a, is able to modulate HSPC fate, it is essential to identify genes regulated by these microRNAs. To address this question, we analyzed Illumina WG6 gene expression arrays from EGFP$^+$ cells transduced with empty vector, miR-cluster, miR-125a and miR-155 (included as a control again). Of the 45.281 probes on the array, 28.977 were expressed in at least 1 of the 4 conditions (empty vector, miR-cluster, miR-125a, and miR-155). For microRNA target prediction, we used one of the most widely used algorithms, namely TargetScan. It predicts 48, 712, and 572 evolutionary conserved targets for miR-99b, let-7e, and miR-125a, respectively.[31] To refine the list, only those targets were selected whose expression reacted on changing microRNA expression levels. In the list of quality-filtered probes (28.977), we identified 912 predicted targets of the entire miR-cluster 99b/let-7e/

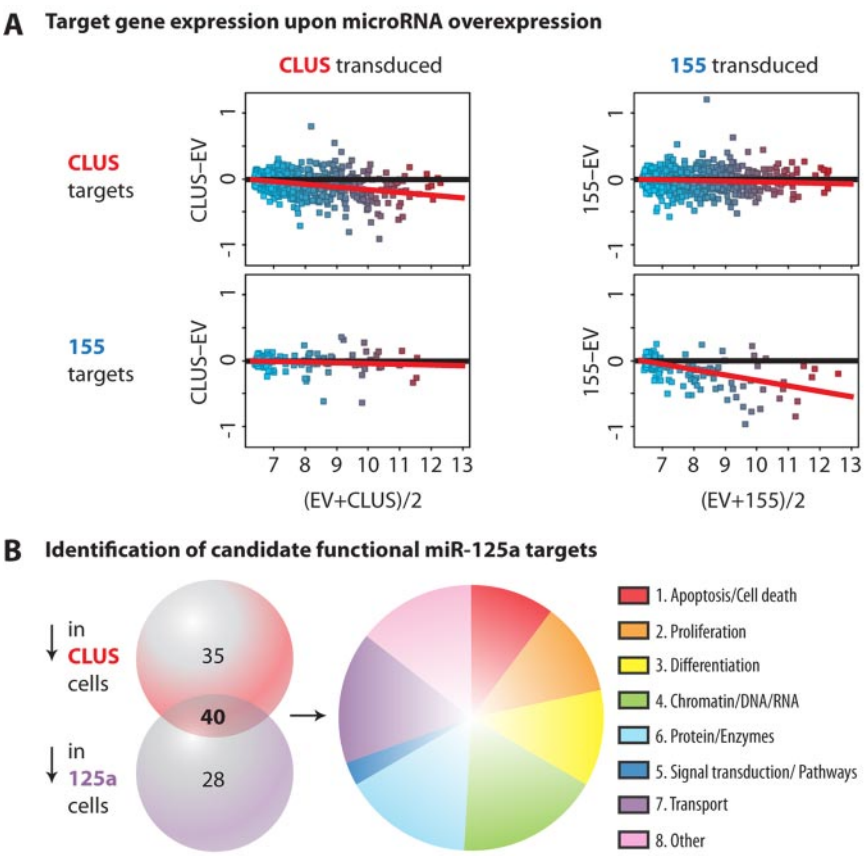

Figure 6. Identification of candidate functional miR-125a targets. (A) Visualization of expression of all quality-filtered predicted miR-cluster and miR-155 targets in miR-cluster–transduced and miR-155–transduced cells. Shown are MvA plots comparing 2 samples. The log2 ratio of each probe (expression difference) is plotted versus the log2 mean for each probe. The red lines represent the best fit to the data. In these plots, the predicted targets that are shared between the miR-cluster and miR-155 are not displayed. (B) Venn diagram showing the identified candidate miR-125a targets down-regulated upon miR-cluster 99b/let-7e/125a or miR-125a overexpression. The intersection represents 40 genes that were consistently 1.5-fold down-regulated upon miR-cluster 99b/let-7e/125a and miR-125a overexpression. These 40 genes were assigned according to Gene Ontology (GO) biological process categories. Genes assigned to common GO categories were grouped together (supplemental Table 3). The pie chart shows relative distributions of grouped GO categories. The size of the sectors in the pie chart was defined based on the number of genes assigned to the category (in redundant fashion). Genes not assigned to any of the defined categories[1-7] were defined as Other.[8] Gene Ontology analyses were performed using GOAL software.[40]

125a, including 485 specific for miR-125a, and 164 targets of miR-155. We then visualized the expression levels of these predicted targets on overexpression of the miR-cluster 99b/let-7e/125a and miR-155 (Figure 6A). This analysis showed that the expression of most of the predicted miR-cluster 99b/let-7e/125a targets was indeed mildly affected in the miR-cluster–transduced cells, but not in the miR-155–transduced cells. In contrast, most of the miR-155 targets were only affected in the miR-155–transduced cells, but not in the miR-cluster–transduced cells. The entire gene expression dataset is available online (supplemental Table 2) and in GEO (accession number GSE33689).

Because our in vitro CAFC activity and in vivo transplantation data indicate that miR-125a is responsible for the majority of the miR-cluster 99b/let-7e/125a–induced phenotypes, we restricted our search for downstream targets to only miR-125a. From the list of predicted miR-125a targets (485, identified using Target Scan), we subsequently selected those probes that were at least 1.5-fold differentially expressed and consistently down-regulated upon overexpression of both miR-cluster 99b/let-7e/125a and miR-125a. This resulted in 45 probes representing 40 genes that qualify as candidate functional targets (Table 1). We classified these 40 potential targets using Gene Ontology functional annotations for biological processes. Annotated categories were grouped as illustrated in Figure 6B (supplemental Table 3). Among these groups were cell proliferation, differentiation, and apoptosis. Seven potential miR-125a targets categorized as apoptosis related. Interestingly, among them was *Bak1*, a proapoptotic gene previously suggested by Guo et al as a miR-125a target. Guo et al showed that miR-125a overexpression phenotypes may be mediated via antiapoptotic effects.[35] This suggests that protection against apoptosis may have been at least partially responsible for the phenotypes that we observed on miR-cluster 99b/let-7e/125a and miR-125a overexpression. However, because enhanced differentiation and lineage skewing were observed in our in vivo transplantations, genes involved in cell proliferation and differentiation may be of importance to explain the full spectrum of effects caused by these microRNAs. Future studies are needed to experimentally validate the candidate functional miR-125a targets.

Discussion

In this report, we set out to determine whether the observed natural variation in HSPC traits across the genetically distinct mouse strains B6 and D2 could be due to natural variation in microRNA expression. We performed a genome-wide microRNA expression study of LSK, LS^-K^+, erythroid and myeloid cells isolated from B6 and D2 mouse strains, and detected natural variation in microRNA expression between these 2 mouse strains. Of special interest was an evolutionary conserved miR-cluster located on chromosome 17 consisting of miR-99b, let-7e, and miR-125a. All cluster members were most highly expressed in LSKs and down-regulated upon differentiation and generally higher expressed in D2 cells compared with B6 cells. We found that overexpression of miR-cluster 99b/let-7e/125a or miR-125a alone conferred an apparent competitive advantage to HSPCs, but also that these cells exhibited increased myeloid differentiation, ultimately leading to the development of MPNs in mice reconstituted with these cells. Loss of competitive advantage following serial transplantation suggests that in the long-term disturbed homeostasis may lead to HSPC exhaustion. Finally, as miR-125a was shown to be responsible for the majority of the miR-cluster 99b/let-7e/125a overexpression phenotypes, we identified candidate functional targets through which miR-125a could modulate HSPC fate.

Table 1. Candidate functional miR-125a targets

		Gene Ontology category							
Gene symbol	**Fold change**	**1**	**2**	**3**	**4**	**5**	**6**	**7**	**8**
Mtf1	−5.11				×				
Alpk3	−4.36								×
Mapk8ip1	−3.92	×			×	×		×	
Bcl11b	−3.81	×	×	×	×				
Ube2r2	−3.6						×		
Mfhas1	−3.6								×
Cnnm1	−3.45							×	
Ets1	−3.4	×	×	×	×				
Taf9b	−3.12	×	×		×				
Cramp1l	−3.11								×
Enpep	−3.09		×						
Ache	−3.01			×				×	
Bmpr2	−2.98		×		×	×			
Celsr2	−2.96			×		×			
Itga9	−2.9					×			
Slc8a2	−2.79							×	
St8sia4	−2.72								×
Smcr8	−2.58								×
Ece1	−2.58	×				×			
Tle3	−2.46			×	×	×			
Ubn1	−2.4			×					
Cdr2l	−2.38								×
Atxn1	−2.37				×	×		×	
Baz2a	−2.31				×				
Asah3l	−2.27		×						
Scn5a	−2.26							×	
Lin28b	−2.19				×				
Pafah1b1	−2.02		×	×				×	
Abcc5	−1.91							×	
Bak1	−1.87	×	×	×	×		×	×	
Coro2a	−1.83								×
Cdc42se1	−1.8					×		×	
Foxq1	−1.79	×			×				
Mtus1	−1.78								×
Stard13	−1.77					×			
Nin	−1.76								×
Tspan12	−1.72					×			
Rhobtb2	−1.63					×			
Pctp	−1.62							×	
Ptpn18	−1.55								×

Fold change indicates down-regulation upon miR-125a overexpression compared to empty vector. Gene Ontology (GO) categories: 1, Apoptosis/cell death; 2, Proliferation; 3, Differentiation; 4, Chromatin/DNA/RNA; 5, Signal transduction/pathways; 6, Protein/enzymes; 7, Transport; and 8, Other (not assigned to categories 1-7).

While we were performing our final experiments, Guo et al reported that miR-99b, let-7e, and miR-125a were enriched in long-term HSCs (LSK/CD34$^-$/Flk2$^-$) and that overexpression of miR-125a alone, but not miR-99b or let-7e, could amplify the HSC pool.[35] This result was shown to be accomplished by decreasing the level of apoptosis in hematopoietic progenitors through targeting proapoptotic genes such as *Bak1*. We confirmed the down-regulation of *Bak1* upon miR-cluster 99b/let-7e/125a and miR-125a overexpression, suggesting that decreased apoptosis of HSPCs may have contributed to the observed hematopoietic phenotypes. In line with this finding was the observed prolonged CAFC activity (day 70) and the initial in vivo competitive advantage in primary recipients, both observed for the miR-cluster and miR-125a–overexpressing cells. However, whereas Guo et al showed amplification of the HSC pool after sustained miR-125a overexpression, we reported a decline of the primitive BM compartment and loss of competitive advantage upon secondary transplantation. Because antiapoptotic effects cannot explain these results, we suggest that additional parameters affecting proliferation and differentiation are contributing to the miR-125a–induced phenotypes. As several identified potential miR-125a targets are involved in cell proliferation and differentiation, it would be interesting to determine their role in miR-cluster 99b/let-7e/125a and miR-125a–mediated hematopoiesis.

Other reports have recently described effects of miR-125b, a paralog of miR-125a, on HSPCs. O'Connell et al[36] and Bousquet et al[37] reported that overexpression of miR-125b caused MPNs that progressed to a lethal acute myeloid leukemia or resulted in B/T-cell acute lymphoblastic leukemia. In addition, Bousquet et al provided evidence that miR-125b confers a proliferative advantage to leukemic cells,[37] whereas O'Connell et al showed that miR-125b promotes hematopoietic engraftment of human HSCs.[36] Finally, Ooi et al reported that overexpression of miR-125b in HSCs enhances their function and enriches for lymphoid-balanced and lymphoid-biased HSCs.[38] They also described a skewing toward the lymphoid lineage in the peripheral blood of these mice, and that a small subset of them developed a lymphoproliferative disease. In addition, they identified *Bmf* and *Klf13* as miR-125b downstream

targets with a link to apoptosis. Whereas in our dataset we could not confirm down-regulation of *Bmf*, *Klf13* was found to be down-regulated upon overexpression of miR-125a and therefore could be considered as a possible candidate.

It is interesting, yet confusing, to see that all the reports on the miR-125 family in HSCs describe distinct gain-of-function phenotypes (from no- to myeloid- to lymphoid malignancies). As suggested by O'Connell et al, differences in overexpression levels may underlie these phenotypic differences.[36] In addition, whereas miR-125a and miR-125b have identical seed sequences, the mature forms of these 2 microRNAs differ. Therefore, it needs to be experimentally validated whether miR-125a and miR-125b really do share the exact same targets.

The initial competitive advantage of miR-cluster 99b/let-7e/125a–overexpressing cells and its loss over time relates to the differences between B6 and D2 mice. First, hematopoietic recovery by B6 and D2 stem cells has been studied in competitive transplantation settings and has uncovered interesting kinetics. Whereas D2 hematopoiesis was predominant initially, it was eclipsed by B6 hematopoiesis over time.[39] Second, 2.6% of B6 stem cells has been shown to be in S-phase of the cell cycle versus a striking 24% of D2 stem cells.[3] Together, these findings indicate that the increased proliferation rate for D2 stem cells may have provided them with an initial competitive advantage, but that this increased cycling rate also made them exhaust more rapidly. We consider it plausible that the differential expression of miR-cluster 99b/let-7e/125a (and thus its targets) may at least be in part responsible for the observed variation in stem cell cycling and repopulation kinetics between B6 and D2 mouse strains.

Collectively, our data and other recent reports point to an important role for the miR-125 family in hematopoiesis. To conclude, we uncovered the existence of natural variation in microRNA expression between mouse strains, and showed that this may contribute to the observed natural variation in HSPC traits. Yet, we were not able to identify any published HSPC traits that mapped to the here-reported locus containing miR-cluster 99b/let-7e/125a.[7] We anticipate that future genetic studies will shed new light on how microRNAs modulate HSPC fate and on how they themselves are regulated.

Acknowledgments

The authors thank Mathilde Broekhuis, Jaring Schreuder, Albertina Ausema, and Bahram Sanjabi for technical assistance; Henk Moes, Geert Mesander, and Roelof Jan van der Lei for assistance in cell sorting; and Brad Dykstra, Joost Kluiver, Anke van den Berg, and Gerwin Huls for scientific advice.

This work was supported by the Dutch Cancer Society (RUG2007-3729), The Netherlands Genomics Initiative (Horizon, 050-71-055), the European Community's Seventh Framework Program (FP7/2007-2013) under grant agreement 222989 (StemExpand), The Netherlands Organization for Scientific Research (VICI, 918-76-601, G.d.H.), and by the European Community (EuroSystem, 200720).

Authorship

Contribution: A.G., M.A.W., R.v.O., L.V.B., and G.d.H. designed research; A.G., M.A.W., S.O., E.W., and M.R. performed research; A.G. and M.A.W. analyzed and interpreted data; E.Z. developed Hemdb.org; and A.G. and M.A.W. wrote the manuscript with contributions from R.v.O., L.V.B., and G.d.H.

Conflict-of-interest disclosure: The authors declare no competing financial interests.

Correspondence: Gerald de Haan, Department of Cell Biology, Section Stem Cell Biology, University Medical Center Groningen, University of Groningen, Groningen 9700 AD, The Netherlands; e-mail: g.de.haan@med.umcg.nl.

References

1. De Haan G, Van Zant G. Intrinsic and extrinsic control of hemopoietic stem cell numbers: mapping of a stem cell gene. *J Exp Med.* 1997;186(4):529-536.
2. De Haan G, Nijhof W, Van Zant G. Mouse strain-dependent changes in frequency and proliferation of hematopoietic stem cells during aging: correlation between lifespan and cycling activity. *Blood.* 1997;89(5):1543-1550.
3. Van Zant G, Eldridge PW, Behringer RR, Dewey MJ. Genetic control of hematopoietic kinetics revealed by analyses of allophenic mice and stem cell suicide. *Cell.* 1983;35(3 pt 2):639-645.
4. Muller-Sieburg CE, Riblet R. Genetic control of the frequency of hematopoietic stem cells in mice: mapping of a candidate locus to chromosome 1. *J Exp Med.* 1996;183(3):1141-1150.
5. Morse HC, III, Chused TM, Hartley JW, et al. Expression of xenotropic murine leukemia viruses as cell-surface gp70 in genetic crosses between strains DBA/2 and C57BL/6. *J Exp Med.* 1979;149(5):1183-1196.
6. Peirce JL, Lu L, Gu J, Silver LM, Williams RW. A new set of BXD recombinant inbred lines from advanced intercross populations in mice. *BMC Genet.* 2004;5:7.
7. Gerrits A, Dykstra B, Otten M, Bystrykh L, De Haan G. Combining transcriptional profiling and genetic linkage analysis to uncover gene networks operating in hematopoietic stem cells and their progeny. *Immunogenetics.* 2008;60(8):411-422.
8. Bystrykh L, Weersing E, Dontje B, et al. Uncovering regulatory pathways that affect hematopoietic stem cell function using 'genetical genomics'. *Nat Genet.* 2005;37(3):225-232.
9. Gerrits A, Li Y, Tesson BM, et al. Expression quantitative trait loci are highly sensitive to cellular differentiation state. *PLoS Genet.* 2009;5(10):e1000692.
10. Bartel DP. MicroRNAs: genomics, biogenesis, mechanism, and function. *Cell.* 2004;116(2):281-297.
11. Ambros V. The functions of animal microRNAs. *Nature.* 2004;431(7006):350-355.
12. Guo H, Ingolia NT, Weissman JS, Bartel DP. Mammalian microRNAs predominantly act to decrease target mRNA levels. *Nature.* 2010;466(7308):835-840.
13. Lim LP, Lau NC, Garrett-Engele P, et al. Microarray analysis shows that some microRNAs down-regulate large numbers of target mRNAs. *Nature.* 2005;433(7027):769-773.
14. Chen CZ, Li L, Lodish HF, Bartel DP. MicroRNAs modulate hematopoietic lineage differentiation. *Science.* 2004;303(5654):83-86.
15. Xiao C, Calado DP, Galler G, et al. MiR-150 controls B cell differentiation by targeting the transcription factor c-Myb. *Cell.* 2007;131(1):146-159.
16. He L, Thomson JM, Hemann MT, et al. A microRNA polycistron as a potential human oncogene. *Nature.* 2005;435(7043):828-833.
17. Xiao C, Srinivasan L, Calado DP, et al. Lymphoproliferative disease and autoimmunity in mice with increased miR-17-92 expression in lymphocytes. *Nat Immunol.* 2008;9(4):405-414.
18. Zhou B, Wang S, Mayr C, Bartel DP, Lodish HF. miR-150, a microRNA expressed in mature B and T cells, blocks early B cell development when expressed prematurely. *Proc Natl Acad Sci U S A.* 2007;104(17):7080-7085.
19. Johnnidis JB, Harris MH, Wheeler RT, et al. Regulation of progenitor cell proliferation and granulocyte function by microRNA-223. *Nature.* 2008;451(7182):1125-1129.
20. Fazi F, Rosa A, Fatica A, et al. A minicircuitry comprised of microRNA-223 and transcription factors NFI-A and C/EBPalpha regulates human granulopoiesis. *Cell.* 2005;123(5):819-831.
21. O'Connell RM, Rao DS, Chaudhuri AA, et al. Sustained expression of microRNA-155 in hematopoietic stem cells causes a myeloproliferative disorder. *J Exp Med.* 2008;205(3):585-594.
22. Thai TH, Calado DP, Casola S, et al. Regulation of the germinal center response by microRNA-155. *Science.* 2007;316(5824):604-608.
23. Rodriguez A, Vigorito E, Clare S, et al. Requirement of bic/microRNA-155 for normal immune function. *Science.* 2007;316(5824):608-611.
24. Esquela-Kerscher A, Slack FJ. Oncomirs-microRNAs with a role in cancer. *Nat Rev Cancer.* 2006;6(4):259-269.
25. Kluiver J, Kroesen BJ, Poppema S, Van den Berg A. The role of microRNAs in normal hematopoiesis and

hematopoietic malignancies. *Leukemia*. 2006;20(11): 1931-1936.

26. Sturn A, Quackenbush J, Trajanoski Z. Genesis: cluster analysis of microarray data. *Bioinformatics*. 2002;18(1):207-208.
27. Mao TK, Chen CZ. Dissecting microRNA-mediated gene regulation and function in T-cell development. *Methods Enzymol*. 2007;427:171-189.
28. Livak KJ, Schmittgen TD. Analysis of relative gene expression data using real-time quantitative PCR and the 2(-Delta Delta C(T)) method. *Methods*. 2001;25(4):402-408.
29. Van Os RP, Dethmers-Ausema B, De Haan G. In vitro assays for cobblestone area-forming cells, LTC-IC, and CFU-C. *Methods Mol Biol*. 2008;430: 143-157.
30. Ploemacher RE, Van der Sluijs JP, Van Beurden CA, Baert MR, Chan PL. Use of limiting-dilution type long-term marrow cultures in frequency analysis of marrow-repopulating and spleen colony-forming hematopoietic stem cells in the mouse. *Blood*. 1991; 78(10):2527-2533.
31. Lewis BP, Burge CB, Bartel DP. Conserved seed pairing, often flanked by adenosines, indicates that thousands of human genes are microRNA targets. *Cell*. 2005;120(1):15-20.
32. Popovic R, Riesbeck LE, Velu CS, et al. Regulation of mir-196b by MLL and its overexpression by MLL fusions contributes to immortalization. *Blood*. 2009;113(14):3314-3322.
33. Zhan M, Miller CP, Papayannopoulou T, Stamatoyannopoulos G, Song CZ. MicroRNA expression dynamics during murine and human erythroid differentiation. *Exp Hematol*. 2007; 35(7):1015-1025.
34. Baskerville S, Bartel DP. Microarray profiling of microRNAs reveals frequent coexpression with neighboring miRNAs and host genes. *RNA*. 2005; 11(3):241-247.
35. Guo S, Lu J, Schlanger R, et al. MicroRNA miR-125a controls hematopoietic stem cell number. *Proc Natl Acad Sci U S A*. 2010;107(32):14229-14234.
36. O'Connell RM, Chaudhuri AA, Rao DS, et al. MicroRNAs enriched in hematopoietic stem cells differentially regulate long-term hematopoietic output. *Proc Natl Acad Sci U S A*. 2010;107(32): 14235-14240.
37. Bousquet M, Harris MH, Zhou B, Lodish HF. MicroRNA miR-125b causes leukemia. *Proc Natl Acad Sci U S A*. 2010;107(50):21558-21563.
38. Ooi AG, Sahoo D, Adorno M, et al. MicroRNA-125b expands hematopoietic stem cells and enriches for the lymphoid-balanced and lymphoid-biased subsets. *Proc Natl Acad Sci U S A*. 2010; 107(50):21505-21510.
39. Van Zant G, Holland BP, Eldridge PW, Chen JJ. Genotype-restricted growth and aging patterns in hematopoietic stem cell populations of allophenic mice. *J Exp Med*. 1990;171(5):1547-1565.
40. Volinia S, Evangelisti R, Francioso F, Arcelli D, Carella M, Gasparini P. GOAL: automated Gene Ontology analysis of expression profiles. *Nucleic Acids Res*. 2004;32(Web Server Issue):W492-W499.